



Reverse-docking study of the organocatalyzed asymmetric Strecker hydrocyanation of aldimines and ketimines

D. Joseph Harriman, Glen F. Deleavey, Andreas Lambropoulos and Ghislain Deslongchamps*

Department of Chemistry, University of New Brunswick, Fredericton, NB, Canada E3B 5A3

Received 26 July 2007; revised 28 September 2007; accepted 2 October 2007

Available online 6 October 2007

Abstract—A methodology for reverse-docking flexible organocatalysts to rigid transition state models of catalyst-free asymmetric reactions has been developed. The investigation of Jacobsen's chiral thiourea-based organocatalyst for the hydrocyanation of aldimines and ketimines (Strecker reaction) via reverse-docking is described. Results from reverse-docking Jacobsen's organocatalyst to both enantiomers of six Strecker TS-models (i.e., rigid transition state models of the catalyst-free asymmetric reaction) indicate a clear energetic preference for binding the organocatalyst to the *R*-enantiomer TS-model, which is in agreement with experimental results. The most favorable docking poses reveal structural features consistent with principles of molecular recognition, catalysis, and NMR data. These poses may represent simplified geometric models of the transition state for the catalyzed reaction.

© 2007 Elsevier Ltd. All rights reserved.

1. Introduction

The rational design of catalysts for carrying out highly enantioselective reactions is of great interest to the chemical community, especially the pharmaceutical industry. Organocatalysts (metal-free organic catalysts) are especially interesting as they present opportunities for biomimicry, and may fall within the realm of 'green chemistry'.¹ In particular, chiral hydrogen-bond donors have emerged as a broadly applicable class of enantioselective organocatalysts.^{2,3}

The hydrocyanation of imines, termed the Strecker reaction, is particularly interesting from an asymmetric catalysis perspective as enantioselectivity is critical for the synthesis of non-natural amino acids.⁴ A study published by Jacobsen and Vachal in 2002⁵ reports the successful application of a flexible thiourea-based organocatalyst for the asymmetric Strecker reaction, using six different imine substrates (four aldimines and two ketimines, Fig. 1). The exact catalytic mechanism for this system remains unknown but is believed to involve hydrogen bonding of both thiourea hydrogens of the catalyst to the imine nitrogen of the substrate. 3D transition state models of catalysis can be highly useful for rationalizing and predicting the stereochemical outcome of asymmetric reactions, and for the design of new catalysts. Computational studies of asymmetric catalysts have been

very useful for in-depth analysis of systems in which the transition state geometries are fairly well defined. However, devising useful transition state models of reactions involving highly flexible organocatalysts presents a particularly daunting challenge; one must explore the vast conformational space of the catalysts as they interact with substrates, approximate their respective transition state geometries and energies, and account for experimental enantioselectivities. For large systems, quantum mechanical (QM) approaches become very computationally demanding, and molecular mechanics (MM) approaches may introduce errors if improperly parameterized force fields are used. However, both QM and MM approaches have enjoyed much success in studying transition state geometries and enantioselectivities of asymmetric reactions.^{6–9}

Computational tools are becoming increasingly useful for both understanding and predicting asymmetric synthesis reactions. Several computational approaches for studying molecular interactions exist, many of which are powerful tools for the organic chemist.¹⁰ Due to the computational demands of QM calculations, a number of docking strategies have been developed based on molecular mechanics principles. The advantage is that MM-based docking algorithms can be used to study systems that are too large to reasonably investigate with QM. We have developed a molecular mechanics-based methodology for reverse-docking flexible organocatalysts to rigid transition state models of catalyst-free asymmetric reactions, producing simplified geometric models of the transition state for the organocatalyzed reactions. Reverse-docking a chiral organocatalyst to two enantiomeric TS-models for a particular substrate produces

Keywords: Asymmetric organocatalysis; Thiourea; Reverse-docking; Strecker reaction.

* Corresponding author. Tel.: +1 506 453 4795; fax: +1 506 453 4981; e-mail: ghislain@unb.ca

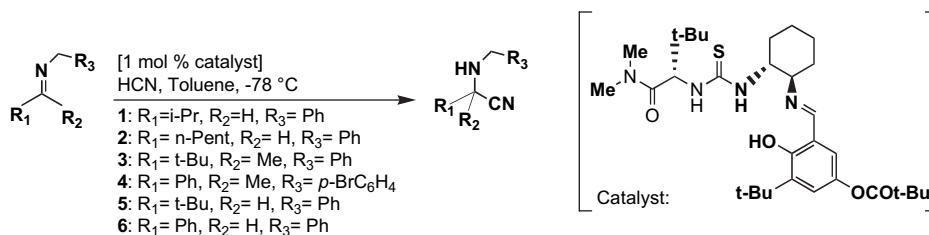


Figure 1. Jacobsen's thiourea-catalyzed Strecker reaction.

approximations of the two enantiomeric transition states, including geometry and relative energy. This reverse-docking approach has predicted the preferred product enantiomer in all cases studied to date.^{11–13} Jacobsen's Strecker organocatalyst offers a particularly challenging case for study due to its large number of conformational rotors. Here, we report the successful reverse-docking investigation of this Strecker reaction, and show that the most energetically favorable docking poses are consistent with experimental data, correctly predicting the preferred product enantiomers and providing modest correlation with the experimental enantiomeric excess (ee) values in some cases.

1.1. Strecker organocatalysis

Jacobsen's organocatalyzed Strecker reaction is believed to involve hydrogen bonding of the thiourea component of the catalyst to the imine nitrogen of the substrates, thus enhancing its electrophilicity toward cyanide addition. NMR data suggests that the system shows an energetic preference for a bifurcated H-bonding pattern, with the imine nitrogen of the substrate hydrogen-bonded to both thiourea hydrogens of the catalyst. Isotope shift experiments also provided evidence that the imine substrate interacts solely with the thiourea hydrogens. Overall the work suggests that: (1) the large group on the imine carbon is directed away from the catalyst and into the solvent; (2) the small group (H or Me) on the imine carbon is aimed directly into the catalyst; (3) the *N*-substituent on the imine is directed away from the catalyst; and (4) HCN addition takes place over the diamino-cyclohexane portion of the catalyst.⁵ Herein, we use the term 'catalytic pose' in reference to a catalyst/TS-model that presents two intermolecular H-bonds between the two thiourea NH groups of the catalyst and the imino nitrogen of the TS-model. This distinction is based not only from the Jacobsen experiments but also from the general role of thioureas in organocatalysis.¹⁴

1.2. Reverse-docking

Traditional docking approaches dock flexible guest molecules within a rigid representation of the host receptor. As one can imagine, host rigidity can be a major source of error, especially in systems demonstrating induced-fit type host-guest interactions. To avoid some of the inherent pitfalls encountered in traditional docking, techniques for reverse-docking are becoming increasingly common.^{11,15,16} The development and preliminary applications of the novel reverse-docking paradigm for studying asymmetric organocatalysis have been previously reported by our group.^{11–13} As shown in Figure 2, typical docking explores the configurational space of a small flexible ligand within the confines

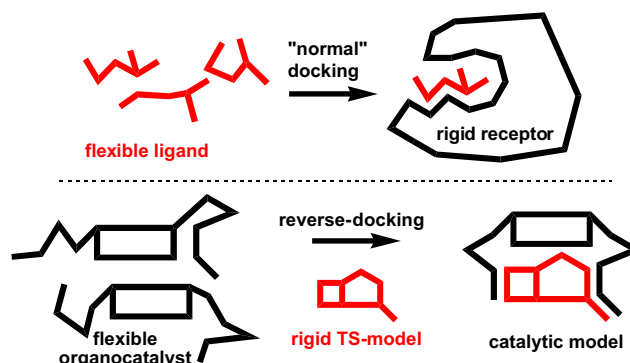


Figure 2. Reverse-docking vs normal docking.

of a large rigid receptor, whereas reverse-docking explores the configurational space of a flexible organocatalyst around rigid transition state models of the catalyst-free asymmetric reaction (referred to as 'TS-models').

This computational approach requires a powerful docking algorithm for adequately sampling the conformational space of flexible organocatalysts around TS-models. Previously, we reported the development of an Energy Minimization-based Docking algorithm, EM-Dock, designed specifically for reverse-docking applications.¹⁷ Written in the Scientific Vector Language (SVL), EM-Dock was implemented in the Molecular Operating Environment (MOE) for rapid prototyping and convenient methodology development.¹⁸ The latest version, EM-Dock 3, performs a systematic conformational search of an organocatalyst using molecular mechanics (MM with energy minimization), and stochastically selects conformers for subsequent reverse-docking to the rigid TS-models. The rigid TS-model geometries are obtained by ab initio calculations, and RESP charges are derived for subsequent MM treatment. As a simple local search strategy, EM-Dock energy minimizes the catalyst/TS-model poses by MM, keeping the TS-model rigid, and a docking score is computed. The chiral organocatalyst is reverse-docked to the two enantiomeric TS-models, and reverse-docking energies are compared.

2. Results and discussion

2.1. Reverse-docking energies

The lowest reverse-docking pose energies, ranks, and calculated enantiomeric excesses (ee) are reported in Table 1 (for information on docking, scoring, and ranking methods, refer to Section 4). In the Jacobsen study, the *R*-enantiomer products were obtained preferentially for both aldimines and

Table 1. Reverse-docking ranks, energies, and calculated enantiomeric excesses

Substrate ^a	'R' TS-model		'S' TS-model		% ee			
	<i>E</i> ^b (rank)	<i>E</i> _{Boltz} ^c	<i>E</i> ^b (rank)	<i>E</i> _{Boltz} ^c	Global ^d	Weighted ^e	Exptl ^f	
1	A	106.95 (1)	106.95	107.62 (1)	107.68	69	61	97
	B	106.95 (1)	107.17	107.62 (1)	107.68			
	C	106.99 (1)	107.29	107.62 (1)	107.72			
2	A	106.25 (1)	106.54	106.52 (1)	106.64	35	23	96
	B	106.27 (1)	106.49	106.53 (1)	106.63			
	C	106.28 (1)	106.46	106.61 (1)	106.76			
3	A	106.30 (1)	106.48	107.46 (1)	107.58	90	85	86
	B	106.36 (1)	106.55	107.47 (2)	107.47			
	C	106.41 (1)	106.68	107.55 (1)	107.61			
4	A	106.10 (1)	106.10	107.58 (1)	107.74	96	98	96
	B	106.11 (1)	106.19	107.65 (1)	107.99			
	C	106.11 (1)	106.28	107.72 (1)	108.03			
5	A	106.54 (1)	106.77	106.66 (1)	106.92	18	20	99.3
	B	106.55 (1)	106.70	106.71 (1)	106.87			
	C	106.58 (1)	106.72	106.73 (1)	106.88			
6	A	106.05 (1)	106.34	107.28 (1)	107.39	92	85	99.3
	B	106.08 (1)	106.36	107.29 (1)	107.29			
	C	106.11 (1)	106.41	107.30 (1)	107.38			

^a Substrates according to Figure 1; rows A–C refer to triplicate reverse-docking runs.

^b Docking energy of lowest-energy database entry (kcal/mol); pose rank in parentheses (1=best rank).

^c Boltzmann-weighted docking energy average.

^d ee Values calculated from the *R/S* docking energy differences at –78 °C using the averaged lowest energies.

^e ee Values calculated from the *R/S* docking energy differences at –78 °C using the Boltzmann-weighted energy averages.

^f Experimental values as reported in Ref. 5.

ketimines. Using the reverse-docking paradigm, one would expect the docking poses of the catalyst around the 'R' TS-models to be lower in energy than for their 'S' enantiomeric counterparts.

The results depicted in Table 1 present a consistent energetic trend favoring the formation of the product *R*-enantiomer, which is in agreement with experimental data. In fact, all six imine TS-models show an energetic preference for the product *R*-enantiomer. The average energy difference between the lowest energy *R*- and *S*-enantiomeric docking poses for the six imine substrates was found to be 0.83 kcal/mol.

For all six substrate TS-models, the lowest energy poses remaining after filtering the *R*-enantiomer databases had a rank of 1, indicating that poses in which H-bonds existed between the catalyst thiourea hydrogens and the imine substrate nitrogen were the most energetically favorable (and potentially relevant for asymmetric catalysis). In contrast, docking to the TS-models leading to formation of the *S*-enantiomer products did not always produce catalytically relevant catalyst conformations as their lowest energy poses. For substrate 3, one of the docking runs to the *S*-enantiomer TS-model produced a lowest energy (107.39 kcal/mol, rank=1) but catalytically 'irrelevant pose', an interesting outcome considering the experimentally observed enantioselectivity.

For both the 'R' and 'S' dockings, the deviations of the triplicate runs were minimal, suggesting that the stochastic sampling of the 'catalytic space' by EM-Dock performs reasonably well. Reproducibility is of utmost importance, not only for identifying the global minima, but also for properly sampling the overall ensemble of docking poses.

The most energetically favorable catalytic poses obtained by EM-Dock 3 not only demonstrate energetic trends in

agreement with experimental data, but the poses themselves reveal a consistent picture. A near-identical set of lowest-energy organocatalyst poses emerges, not only within any triplicate run, but also when comparing TS-models 1–6 within the same enantiomeric series. Furthermore, the catalyst poses around the 'R' TS-models are consistent with the catalytic model advanced by Jacobsen, lending support for our computational approach. Figure 3 depicts the most energetically favorable catalyst poses around the 'R' and 'S' TS-models of aldimine 1; these poses are nearly identical to those obtained when docking to the TS-models of aldimines 2, 5, and 6.

Figure 4 depicts the most energetically favorable catalyst poses around the 'R' and 'S' TS-models of ketimine 3; these poses are nearly identical to those obtained when docking to the TS-models of ketimine 4. Both Figures 3 and 4 reveal bifurcated H-bonding of the thiourea hydrogens to the imino nitrogen in the catalytic models, which is consistent with the theorized mode of catalysis. For the preferred 'R' TS-model docking poses, the isopropyl and *t*-butyl groups on the imine carbons are directed away from the catalyst and into the solvent, the hydrogen and methyl groups on the imine carbons are aimed toward the catalyst, the benzyl groups on the imine nitrogens are directed away from the catalyst, and the CN[–] addition is taking place over the diaminocyclohexane portion of the catalyst. We believe these basic spatial features of the docking poses are consistent with the Jacobsen model.

The 'S' catalytic model, while showing general features similar to the 'R' counterpart, is complexed to the imine in a different spatial orientation, and is higher in energy, resulting in the enantioselectivity trend of the docking results.

While the reverse-docking simulations produced by EM-Dock 3 were able to accurately predict the enantiomeric trends, these methods currently offer only a qualitative

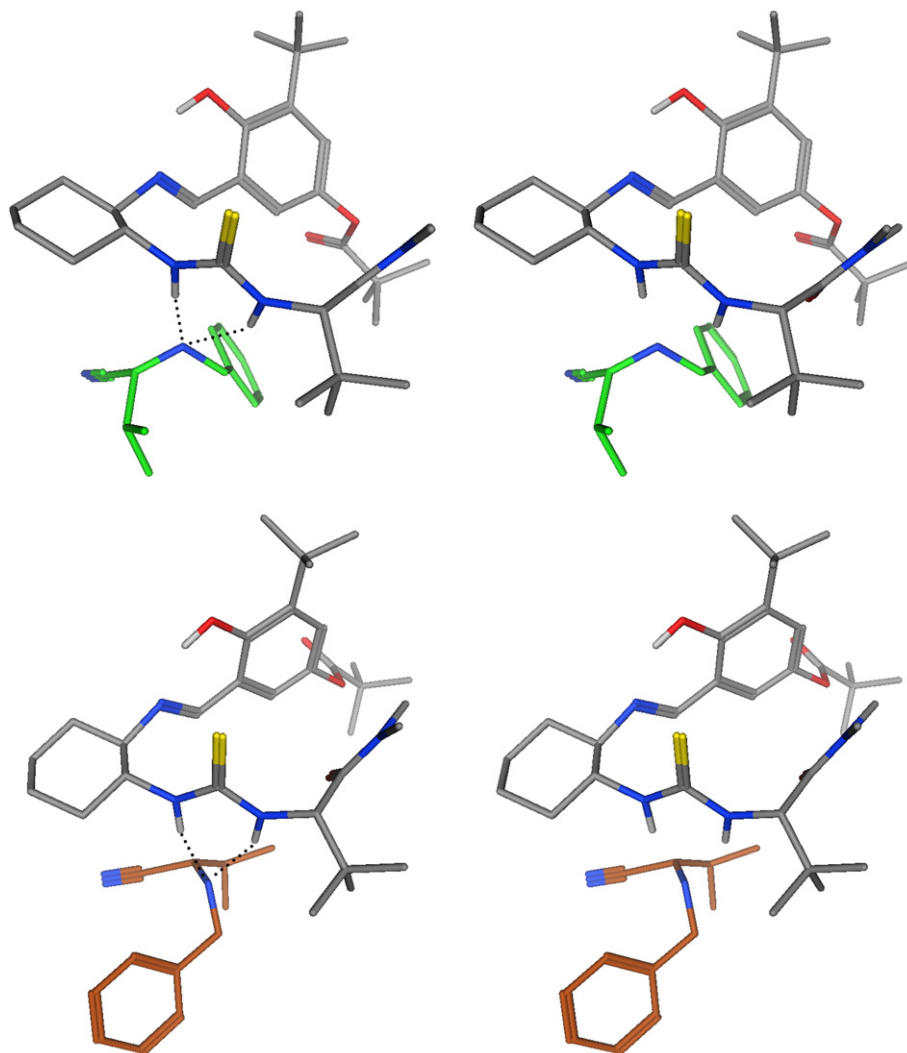


Figure 3. Stereoviews of the best reverse-docking poses for aldimine substrate **1**. Non-polar hydrogens were omitted for clarity; *top*: ‘*R*’ TS-model ($E=106.95$ kcal/mol, rank=1); *bottom*: ‘*S*’ TS-model ($E=107.62$ kcal/mol, rank=1).

enantiomeric comparison. Table 1 compares the calculated enantiomeric excess values to the experimental values. The average energy difference between the lowest energy ‘*R*’ and ‘*S*’ dockings for the series of six enantiomeric TS-model pairs is 0.83 kcal/mol, corresponding to a 79% ee at -78 °C. Using the Boltzmann-weighted averages instead of the global energy minima yields a calculated energy difference of 0.73 kcal/mol, corresponding to a 74% ee at -78 °C. While the ee values produced from the Boltzmann-weighted average energies are not as good as those produced from the global minima, the enantioselectivity trends are still clear. Interestingly, the Boltzmann-weighted energies are very similar within triplicate docking attempts, indicating that EM-Dock 3 is effective at generating similar ensembles of reverse-docking poses.

While EM-Dock 3 was generally able to produce ee close to the experimental values for some of the substrates, overall these results do not correlate completely with the 1.00–2.19 kcal/mol energy difference required to produce the experimental 86–99.3% ee values. Notwithstanding, these results are extremely encouraging, as the calculated ee values are in the proper range despite being very sensitive

to small energy differences at the transition states. In the end, the consistent energetic preference for the *R*-enantiomer of all six TS-models suggests that the energetic differences are indeed significant and warrant further investigations and methodology development.

For the ‘*S*’ TS-models, some catalyst poses showing thiourea H-bonding to the CN^- group instead of the imino nitrogen appeared in the top 1–5 ranks of some of the docking results. These poses represent transition state models where the catalyst H-bonds to the cyanide component of the TS-model as the only obvious intermolecular interaction and bears no electrophilic activation of the imine. This is certainly an artifact of the rigid TS-model approach. These artifactual poses are easily filtered out of the databases.

Substrate **5** shows only a 0.12 kcal/mol energy difference between enantiomers, which is substantially lower than the experimental value. Visual inspection of the docking poses did not reveal a clear reason for this outcome.

One of the ‘*S*’ TS-model docking results for substrate **3** yielded a global minimum that did not correspond to

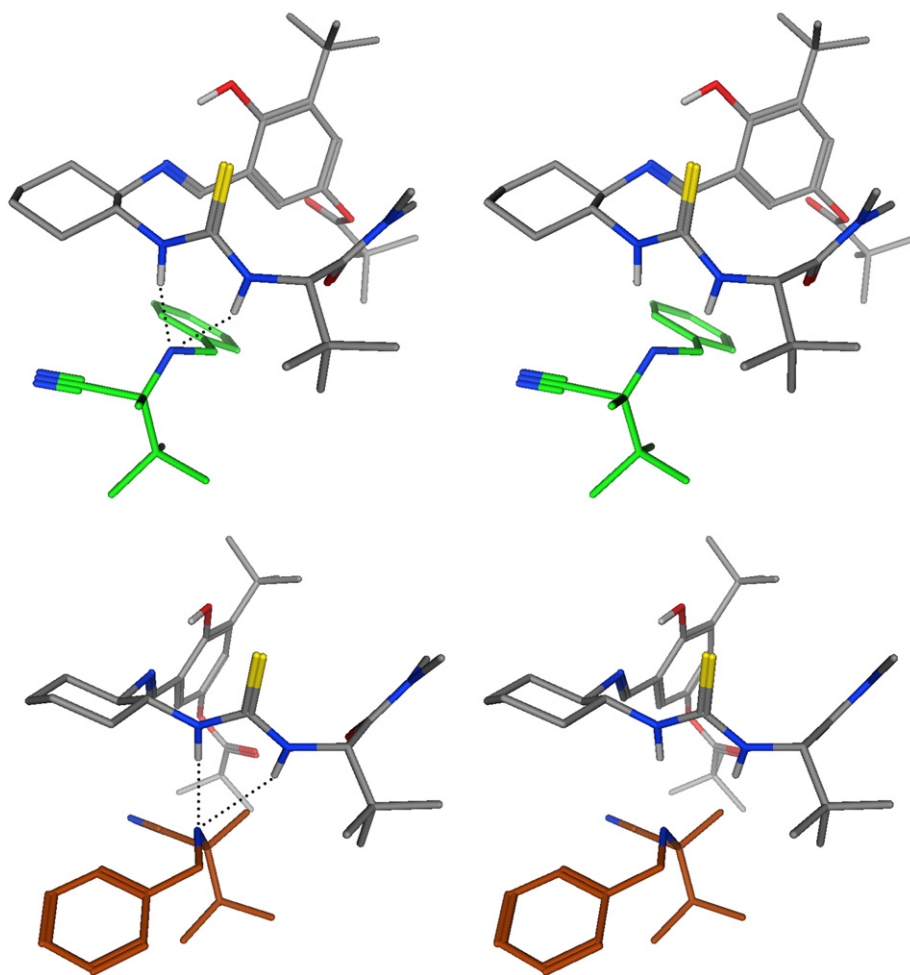


Figure 4. Stereoviews of the best reverse-docking poses for ketimine substrate **3**. Non-polar hydrogens were omitted for clarity; *top*: ‘*R*’ TS-model ($E=106.30$ kcal/mol, rank=1); *bottom*: ‘*S*’ TS-model ($E=107.46$ kcal/mol, rank=1).

a ‘catalytic pose’ (i.e., two proper intermolecular H-bonds); the anticipated catalytic pose appeared as the #2 ranked pose. Further analysis revealed that the best ranking pose had the thiourea group in a *cis*–*trans* conformation rather than the catalytic *trans*–*trans* conformation observed for the other substrates. This result was interesting in light of a recently reported study¹⁸ showing that, among a series of *N,N'*-dialkylthioureas, the *cis*–*trans* conformation of *N,N'*-diisopropylthiourea is only slightly more stable than the *trans*–*trans* conformation (0.1 kcal/mol). This thiourea is essentially isosteric to the thiourea component of Jacobsen’s Strecker catalyst.

Our work reveals an energetic preference for the *trans*–*trans* catalyst conformation bound to the ‘*R*’ TS-models, suggestive of an induced-fit where the catalyst may interact in a catalytically productive manner, adopting a slightly higher energy *trans*–*trans* geometry. Bearing this in mind, it is interesting to note that some of our ‘*S*’ poses are less capable of adopting *trans*–*trans* ‘catalytic’ conformations.

Although the reverse-docking results for all 12 imine TS-models demonstrate a clear energetic trend favoring the formation of the ‘*R*’ products, we are still mindful that, in its current form, the method is still a qualitative investigational tool. A simple MM-based approach for computing

molecular interactions is used. TS models were created based on the theory that catalyst H-bonding stabilizes the incipient negative charge that develops on the imino nitrogen during direct cyanide addition. The methodology assumes identical enantiomeric TS-models interacting with the chiral catalyst. It does not allow for changes in TS-model geometry upon catalyst binding. It ignores the energy contribution for raising the bound catalyst to a proper transition state geometry, as well as entropic effects, assuming that the entropy decrease of the catalyst upon binding to the TS-model is the same for all bound conformations. Solvent effects are treated in the most rudimentary way.

3. Conclusions

In summary, a methodology for reverse-docking flexible organocatalysts to rigid transition state models of catalyst-free asymmetric reactions (TS-models) has been developed and applied to Jacobsen’s Strecker organocatalyst. The resulting reverse-docking poses were treated as simplified models for the catalyzed transition state of the Strecker reaction. Molecular mechanics-based energy calculations, scoring, and ranking of the reverse-docking poses revealed clear energetic trends favoring the formation of the *R*-enantiomer product for all six of the imine substrates studied, in

agreement with experimental values. Structural analysis of the reverse-docking poses determined that the most energetically favorable catalytically relevant poses had the same structural features as experimental NMR data, including bifurcated H-bonding a key feature of catalysis. Relative docking energies for the series of six enantiomeric TS-model pairs, using the global energy minima, gave an average difference of 0.83 kcal/mol, corresponding to a 79% ee. Using the Boltzmann-weighted averages of the docking ensembles returned an average difference of 0.73 kcal/mol, corresponding to a 74% ee. These values are in rough agreement with experimental values. EM-Dock 3 has emerged as an interesting tool for investigating enantioselective organocatalysis, and for producing reasonable 3D transition state models for these reactions. Further studies are currently underway to address simplifications inherent in the original methodology, to improve ee predictions, and to improve general usability. It is our hope that this may become an important tool for the rational design of asymmetric organocatalysts and other nano-molecular devices.

4. Computational methods

4.1. Catalyst modeling

The thiourea-based catalyst shown in Figure 1 was modeled in MOE 2005.06¹⁹ using the MMFF94x forcefield.²⁰ The structure was re-optimized at the HF/6-31G* level in Gaussian 03²¹ and RESP charges²² were fitted using Antechamber (Amber 7 package).²³

4.2. Hydrocyanation TS modeling

The catalyst-free transition states for cyanide addition to the six imine substrates reported in Figure 1 (*Z*-isomers, vide infra) were modeled initially using MMFF94x. As an initial estimate for the TS structures, the incipient C⋯N addition bonds were restrained to 2.0 Å during the conformational search and accompanying energy minimization. The lowest energy conformation for each was used as input for subsequent transition state searches at the HF/6-31G* level, which is appropriate for the ensuing RESP charge calculations. Initial force constants at the starting geometry were calculated using the same basis set as the optimization. All optimized structures were subjected to a frequency calculation to ascertain stationary points along the potential energy surface; the number of negative eigen values was examined to determine if geometries corresponded to a first-order saddle point. RESP charges were subsequently calculated using Antechamber. Mirror inversion produced six pairs of enantiomeric TS-models.

With the Jacobsen catalyst, only the *Z*-imine isomers are reported to undergo enantioselective hydrocyanation even though the *E*-isomer is typically lower in energy. To avoid user bias, both the *Z*- and *E*-imine TS-models (*R* and *S* enantiomers) were modeled and used in the initial reverse-docking experiments. Results showed that *Z*-isomers consistently showed dual H-bonding of the imine nitrogen to the thiourea group of the catalyst. However, the *E*-imine complexes showed no such pattern and only one H-bond at best. Based on this notion, and the NMR data, all subsequent reverse-docking simulations were carried out on the *Z*-imines only.

4.3. Reverse-docking

Using EM-Dock 3, the following input values were found to be the best compromise between accuracy and computation time: runs: 500; screening attempts: 1000; cutoff value: 20; docking box: 180×180×180 Å; rotatable bonds: eight relevant rotatable bonds were retained for the conformational search (excluded *t*-butyl rotations, cyclohexyl chair inversion, and benzaldimine rotation due to intramolecular H-bonding to the *ortho*-phenol group); solvation: distance dependent; dielectric constant: 1.

Each of the 12 reverse-dockings were carried out in triplicate: 500 run EM-Dock jobs typically require 30 h to compute on a 2.8 GHz Intel Xeon processor, followed by another 3 h for energy minimization and database processing. To ensure that the docking space was being adequately sampled by the 500 run simulations, a single 5000 run simulation was completed for each of the 12 substrates (18 days of calculation per run), none returning lower energy poses than the 500 run simulations. All docking poses were energy minimized around their respective rigid TS-models using the same parameters used in the initial reverse-docking process except that the solvent dielectric constant was set to 2.4 to incorporate bulk electrostatic dampening properties of toluene.

4.4. Data processing

The databases of reverse-docking poses were scored as a sum of the potential energy of the catalyst plus the intermolecular interaction energies (electrostatic and van der Waals) between catalyst and TS-models with MMFF94x. Attempts to score poses using single point QM calculations were also made, but without the prohibitively time-consuming QM optimization steps before energy calculations, this approach proved inconsistent and error prone. The poses were ranked by energy, 1 corresponding to the lowest (best) energy score. Each database was filtered to eliminate poses in which intermolecular H_{thiourea}⋯N_{imine} distances were greater than 4 Å. The overall ranks, determined before filtering, were retained for analysis and discussion, serving as indicators of whether the pose filtering removed any energetically relevant docking poses. Duplicate entries were deleted from each database using a 0.3 Å RMSD distance cutoff, as well as poses >2.7 kcal/mol higher than their respective global minima. The Boltzmann weights of each database entry were calculated (at −78 °C) based on the pose energies, poses representing less than 5% of the Boltzmann population were deleted, and the Boltzmann-weighted energy averages were calculated.

Acknowledgements

Financial support from the Natural Sciences and Engineering Research Council, the New Brunswick Innovation Foundation, and the University of New Brunswick is gratefully acknowledged. We are also grateful to the Chemical Computing Group Inc. for software licenses and SVL support.

Supplementary data

Cartesian coordinates for TS-models and optimized catalyst/TS-model docking poses, including docking energies.

Supplementary data associated with this article can be found in the online version, at doi:10.1016/j.tet.2007.10.009.

References and notes

1. Anastas, P. T.; Bartlett, L. B.; Kirchoff, M. M.; Williamson, T. C. *Catal. Today* **2000**, *55*, 11.
2. Taylor, M. S.; Jacobsen, E. N. *Angew. Chem., Int. Ed.* **2006**, *45*, 1520.
3. Dalko, P. I.; Moisan, L. *Angew. Chem., Int. Ed.* **2004**, *43*, 5138.
4. Beller, M.; Eckert, M.; Geissler, H.; Napierski, B.; Rebenstock, H.-P.; Holla, E. W. *Chem.—Eur. J.* **1998**, *4*, 935.
5. Vachal, P.; Jacobsen, E. N. *J. Am. Chem. Soc.* **2002**, *124*, 10012.
6. Ragusa, A.; Hayes, J. M.; Light, M. E.; Kilburn, J. D. *Eur. J. Org. Chem.* **2006**, *16*, 3545.
7. Kozlowski, M. C.; Dixon, S. L.; Panda, M.; Lauri, G. *J. Am. Chem. Soc.* **2003**, *125*, 6614.
8. Wiberg, K. B.; Bailey, W. F. *J. Am. Chem. Soc.* **2001**, *123*, 8231.
9. Gordillo, R.; Dudding, T.; Anderson, C. D.; Houk, K. N. *Org. Lett.* **2007**, *9*, 501.
10. Lipkowitz, K. B.; Kozlowski, M. C. *Synlett* **2003**, 1547.
11. Harriman, D. J.; Deslongchamps, G. *J. Comput.-Aided Mol. Des.* **2004**, *18*, 303.
12. Harriman, D. J.; Deslongchamps, G. *J. Mol. Model.* **2006**, *12*, 793.
13. Harriman, D. J.; Lambropoulos, A.; Deslongchamps, G. *Tetrahedron Lett.* **2007**, *48*, 689.
14. Connon, S. J. *Chem.—Eur. J.* **2006**, *12*, 5418.
15. Kamper, A.; Apostolakis, J.; Rarey, M.; Marian, C. M.; Lengauer, T. *J. Chem. Inf. Model.* **2006**, *46*, 903.
16. Li, H.; Gao, Z.; Kang, L.; Zhang, H.; Yang, K.; Yu, K.; Luo, X.; Zhu, W.; Chen, K.; Shen, J.; Wang, X.; Jiang, H. *Nucleic Acids Res.* **2006**, *34*, W219.
17. Wiley, E. A.; MacDonald, M.; Lambropoulos, A.; Harriman, D. J.; Deslongchamps, G. *Can. J. Chem.* **2006**, *84*, 384.
18. Custelcean, R.; Gorbunova, M. G.; Bonnesen, P. V. *Chem.—Eur. J.* **2005**, *11*, 1459.
19. Chemical Computing Group, 2006.
20. Halgren, T. A. *J. Comput. Chem.* **1999**, *20*, 730.
21. Frisch, M. J.; Trucks, G. W.; Schlegel, H. B.; Scuseria, G. E.; Robb, M. A.; Cheeseman, J. R.; Montgomery, J. A., Jr.; Vreven, T.; Kudin, K. N.; Burant, J. C.; Millam, J. M.; Iyengar, S. S.; Tomasi, J.; Barone, V.; Mennucci, B.; Cossi, M.; Scalmani, G.; Rega, N.; Petersson, G. A.; Nakatsuji, H.; Hada, M.; Ehara, M.; Toyota, K.; Fukuda, R.; Hasegawa, J.; Ishida, M.; Nakajima, T.; Honda, Y.; Kitao, O.; Nakai, H.; Klene, M.; Li, X.; Knox, J. E.; Hratchian, H. P.; Cross, J. B.; Bakken, V.; Adamo, C.; Jaramillo, J.; Gomperts, R.; Stratmann, R. E.; Yazyev, O.; Austin, A. J.; Cammi, R.; Pomelli, C.; Ochterski, J. W.; Ayala, P. Y.; Morokuma, K.; Voth, G. A.; Salvador, P.; Dannenberg, J. J.; Zakrzewski, V. G.; Dapprich, S.; Daniels, A. D.; Strain, M. C.; Farkas, O.; Malick, D. K.; Rabuck, A. D.; Raghavachari, K.; Foresman, J. B.; Ortiz, J. V.; Cui, Q.; Baboul, A. G.; Clifford, S.; Cioslowski, J.; Stefanov, B. B.; Liu, G.; Liashenko, A.; Piskorz, P.; Komaromi, I.; Martin, R. L.; Fox, D. J.; Keith, T.; Al-Laham, M. A.; Peng, C. Y.; Nanayakkara, A.; Challacombe, M.; Gill, P. M. W.; Johnson, B.; Chen, W.; Wong, M. W.; Gonzalez, C.; Pople, J. A. *Gaussian 03*; Gaussian: Wallingford, CT, 2004.
22. Bayly, C.; Cieplak, P.; Cornell, W.; Kollman, P. *J. Phys. Chem.* **1993**, *97*, 10269.
23. Case, D. A.; Pearlman, D. A.; Caldwell, J. W.; Cheatham, T. E., III; Wang, J.; Ross, W. S.; Simmerling, C. L.; Darden, T. A.; Merz, K. M.; Stanton, R. V.; Cheng, A. L.; Vincent, J. J.; Crowley, M.; Tsui, V.; Gohlke, H.; Radmer, R. J.; Duan, Y.; Pitera, J.; Massova, I.; Seibel, G. L.; Singh, U. C.; Weiner, P. K.; Kollman, P. A. *AMBER 7*; University of California: San Francisco, CA, 2002.